



2011-03

# Blind equalization and fading channel signal recovery of OFDM modulation

Stranges, Anthony G.

Monterey, California. Naval Postgraduate School

---

<http://hdl.handle.net/10945/5740>



Calhoun is a project of the Dudley Knox Library at NPS, furthering the precepts and goals of open government and government transparency. All information contained herein has been approved for release by the NPS Public Affairs Officer.

**Dudley Knox Library / Naval Postgraduate School**  
**411 Dyer Road / 1 University Circle**  
**Monterey, California USA 93943**

<http://www.nps.edu/library>



# NAVAL POSTGRADUATE SCHOOL

MONTEREY, CALIFORNIA

## THESIS

**BLIND EQUALIZATION AND FADING CHANNEL  
SIGNAL RECOVERY OF OFDM MODULATION**

by

Anthony G. Stranges

March 2011

Thesis Co-Advisors:

Roberto Cristi  
Frank Kragh

**Approved for public release; distribution is unlimited**

THIS PAGE INTENTIONALLY LEFT BLANK

<b>REPORT DOCUMENTATION PAGE</b>			<i>Form Approved OMB No. 0704-0188</i>	
Public reporting burden for this collection of information is estimated to average 1 hour per response, including the time for reviewing instruction, searching existing data sources, gathering and maintaining the data needed, and completing and reviewing the collection of information. Send comments regarding this burden estimate or any other aspect of this collection of information, including suggestions for reducing this burden, to Washington headquarters Services, Directorate for Information Operations and Reports, 1215 Jefferson Davis Highway, Suite 1204, Arlington, VA 22202-4302, and to the Office of Management and Budget, Paperwork Reduction Project (0704-0188) Washington DC 20503.				
<b>1. AGENCY USE ONLY (Leave blank)</b>		<b>2. REPORT DATE</b> March 2011	<b>3. REPORT TYPE AND DATES COVERED</b> Master's Thesis	
<b>4. TITLE AND SUBTITLE</b> Blind Equalization and Fading Channel Signal Recovery of OFDM Modulation			<b>5. FUNDING NUMBERS</b>	
<b>6. AUTHOR(S)</b> Anthony G. Stranges			<b>8. PERFORMING ORGANIZATION REPORT NUMBER</b>	
<b>7. PERFORMING ORGANIZATION NAME(S) AND ADDRESS(ES)</b> Naval Postgraduate School Monterey, CA 93943-5000			<b>10. SPONSORING/MONITORING AGENCY REPORT NUMBER</b>	
<b>9. SPONSORING /MONITORING AGENCY NAME(S) AND ADDRESS(ES)</b> N/A			<b>11. SUPPLEMENTARY NOTES</b> The views expressed in this thesis are those of the author and do not reflect the official policy or position of the Department of Defense or the U.S. Government. IRB Protocol number _____N/A_____.	
<b>12a. DISTRIBUTION / AVAILABILITY STATEMENT</b> Approved for public release; distribution is unlimited			<b>12b. DISTRIBUTION CODE</b>	
<b>13. ABSTRACT</b>  Algorithms for blind equalization and data recovery of orthogonal frequency-division multiplexed (OFDM) signals transmitted through fading channels are implemented and simulated in this thesis. The channel is estimated without knowledge of the transmitted sequence (i.e., blindly) using a least mean squares (LMS) adaptive filter and filter bank precoders. This method was used to estimate channel characteristics using both binary and quadrature phase-shift keying signals. Additionally, the method was analyzed for robustness with a poor initial estimate of channel characteristics, with the addition of white Gaussian noise to the signal, and with non-stationary channel conditions.  In addition, it is shown that the proposed method is particularly suited in situations with deep fading channels, where some of the subcarriers have a very low SNR.  Simulations for both aspects of this thesis were conducted using MATLAB, and the results are presented.				
<b>14. SUBJECT TERMS</b>  OFDM, LMS, Blind Equalization, Fading Channels			<b>15. NUMBER OF PAGES</b>  69	
			<b>16. PRICE CODE</b>	
<b>17. SECURITY CLASSIFICATION OF REPORT</b>  Unclassified	<b>18. SECURITY CLASSIFICATION OF THIS PAGE</b>  Unclassified	<b>19. SECURITY CLASSIFICATION OF ABSTRACT</b>  Unclassified	<b>20. LIMITATION OF ABSTRACT</b>  UU	

THIS PAGE INTENTIONALLY LEFT BLANK

**Approved for public release; distribution is unlimited**

**BLIND EQUALIZATION AND FADING CHANNEL SIGNAL RECOVERY OF  
OFDM MODULATION**

Anthony G. Stranges  
Lieutenant, United States Navy  
B.S., United States Naval Academy, 2004

Submitted in partial fulfillment of the  
requirements for the degree of

**MASTER OF SCIENCE IN ELECTRICAL ENGINEERING**

from the

**NAVAL POSTGRADUATE SCHOOL  
March 2011**

Author: Anthony G. Stranges

Approved by: Roberto Cristi  
Thesis Co-Advisor

Frank Kragh  
Thesis Co-Advisor

R. Clark Robertson  
Chair, Department of Electrical and Computer Engineering

THIS PAGE INTENTIONALLY LEFT BLANK

## **ABSTRACT**

Algorithms for blind equalization and data recovery of orthogonal frequency-division multiplexed (OFDM) signals transmitted through fading channels are implemented and simulated in this thesis. The channel is estimated without knowledge of the transmitted sequence (i.e., blindly) using a least mean squares (LMS) adaptive filter and filter bank precoders. This method was used to estimate channel characteristics using both binary and quadrature phase-shift keying signals. Additionally, the method was analyzed for robustness with a poor initial estimate of channel characteristics, with the addition of white Gaussian noise to the signal, and with non-stationary channel conditions.

In addition, it was shown that the proposed method is particularly suited in situations with deep fading channels, where some of the subcarriers have a very low signal-to-noise ratio (SNR).

Simulations for both aspects of this thesis were conducted using MATLAB, and the results are presented.



THIS PAGE INTENTIONALLY LEFT BLANK

# TABLE OF CONTENTS

<b>I.</b>	<b>INTRODUCTION.....</b>	<b>1</b>
<b>A.</b>	<b>BACKGROUND .....</b>	<b>1</b>
<b>B.</b>	<b>OBJECTIVES AND METHODOLOGY .....</b>	<b>1</b>
<b>C.</b>	<b>BENEFITS OF STUDY .....</b>	<b>2</b>
<b>D.</b>	<b>ORGANIZATION .....</b>	<b>2</b>
<b>II.</b>	<b>OVERVIEW OF OFDM .....</b>	<b>3</b>
<b>A.</b>	<b>OFDM SYMBOL .....</b>	<b>4</b>
<b>B.</b>	<b>OFDM IN STANDARDS .....</b>	<b>7</b>
<b>1.</b>	<b>IEEE Standard 802.11a .....</b>	<b>7</b>
<b>2.</b>	<b>IEEE Standard 802.11g.....</b>	<b>8</b>
<b>3.</b>	<b>IEEE Standard 802.11n.....</b>	<b>8</b>
<b>4.</b>	<b>Other Standards.....</b>	<b>8</b>
<b>III.</b>	<b>BLIND CHANNEL ESTIMATION IN OFDM WITH ZERO PREFIX.....</b>	<b>11</b>
<b>A.</b>	<b>BLIND EQUALIZATION USING A ZERO PREFIX.....</b>	<b>11</b>
<b>B.</b>	<b>CHANNEL ESTIMATION.....</b>	<b>12</b>
<b>1.</b>	<b>Received OFDM Symbol .....</b>	<b>13</b>
<b>2.</b>	<b>Channel Estimation from a Block of Received Data .....</b>	<b>15</b>
<b>IV.</b>	<b>RECURSIVE IMPLEMENTATION.....</b>	<b>21</b>
<b>A.</b>	<b>OFDM WITH CYCLIC PREFIX AND OFDM WITH ZERO PREFIX.....</b>	<b>21</b>
<b>B.</b>	<b>PROPOSED APPROACH .....</b>	<b>22</b>
<b>C.</b>	<b>SIMULATION RESULTS .....</b>	<b>24</b>
<b>1.</b>	<b>Performance in the Presence of Multipath and AWGN.....</b>	<b>25</b>
<b>2.</b>	<b>Non-Stationary Channel Performance .....</b>	<b>28</b>
<b>3.</b>	<b>Effects of Errors in the Initial Channel Estimate .....</b>	<b>30</b>
<b>V.</b>	<b>DATA RECOVERY FROM A FADED SUBCARRIER.....</b>	<b>35</b>
<b>A.</b>	<b>PROPOSED NULL ESTIMATION METHOD .....</b>	<b>35</b>
<b>B.</b>	<b>SIMULATION RESULTS .....</b>	<b>37</b>
<b>VI.</b>	<b>CONCLUSION .....</b>	<b>41</b>
<b>A.</b>	<b>SUMMARY .....</b>	<b>41</b>
<b>B.</b>	<b>SIGNIFICANT RESULTS.....</b>	<b>41</b>
<b>C.</b>	<b>RECOMMENDATIONS FOR FUTURE WORK.....</b>	<b>43</b>
	<b>LIST OF REFERENCES.....</b>	<b>45</b>
	<b>INITIAL DISTRIBUTION LIST .....</b>	<b>47</b>

THIS PAGE INTENTIONALLY LEFT BLANK

## LIST OF FIGURES

Figure 1.	A block diagram of a simple OFDM communications system. From [4].	6
Figure 2.	Mapping of IFFT inputs to time-domain outputs for 802.11a. From [7].	8
Figure 3.	The signal $\underline{s}[n]$ is encoded with the $R_1$ matrix, then $L$ zeros are appended. After [7].	12
Figure 4.	A delay of $M$ points results in a phase shift of the first OFDM symbol with a ZP and new symbols subsequent to that.	21
Figure 5.	QPSK SER versus SNR with a step size of $\mu = 10^{-7}$ .	26
Figure 6.	QPSK SER versus SNR with a step size of $\mu = 3 \times 10^{-5}$ .	27
Figure 7.	QPSK SER versus random walk step size with an LMS step size of $\mu = 3 \times 10^{-5}$ .	29
Figure 8.	A comparison of the block and proposed adaptive method of calculating the channel using a step size of $\mu = 3 \times 10^{-5}$ . These results were generated using 500 trials at each data point.	30
Figure 9.	Number of OFDM symbols required to converge versus seed channel variance for a step size of $\mu = 10^{-7}$ .	31
Figure 10.	Number of OFDM symbols required to converge versus seed channel variance for a step size of $\mu = 3 \times 10^{-5}$ .	32
Figure 11.	One of a family of channel frequency responses, all having nulls at $\omega = 0.589$ radians.	38
Figure 12.	A comparison of the QPSK symbol error rate between a normal OFDM receiver algorithm and a null estimating OFDM receiver algorithm.	39

THIS PAGE INTENTIONALLY LEFT BLANK

## LIST OF TABLES

Table 1.	Comparison of calculated SER at various SNR for the blind estimation methods using a step size of $\mu = 10^{-7}$ .....42
Table 2.	Comparison of convergence speed for various seed channel variances for the original and alternative adaptive methods with an LMS step size of $\mu = 3 \times 10^{-5}$ .....43

THIS PAGE INTENTIONALLY LEFT BLANK

## LIST OF ACRONYMS AND ABBREVIATIONS

AWGN	Additive White Gaussian Noise
BPSK	Binary Phase-Shift Keying
CP	Cyclic Prefix
DFT	Discrete Fourier Transform
FFT	Fast Fourier Transform
IDFT	Inverse Discrete Fourier Transform
IFFT	Inverse Fast Fourier Transform
ISI	Inter-Symbol Interference
LMS	Least Mean Square
LTI	Linear Time Invariant
MIMO	Multiple-Input Multiple-Output
OFDM	Orthogonal Frequency-Division Multiplexing
QPSK	Quadrature Phase-Shift Keying
SER	Symbol Error Rate
SNR	Signal to Noise Ratio
ZP	Zero Prefix



THIS PAGE INTENTIONALLY LEFT BLANK

## EXECUTIVE SUMMARY

Orthogonal frequency-division multiplexing (OFDM) modulation has become the preferred modulation method for numerous modern standards, from IEEE 802.11a/g/n (Wi-Fi) to IEEE 802.16 (WiMAX) to 4G Long Term Evolution [1]. The reason that OFDM modulation has become so prevalent is because of a number of advantages it has over other modulation techniques.

One of the main advantages of OFDM modulation is the ease of channel equalization, especially in multipath environments [1]. This is achieved by dividing the channel bandwidth into narrow sub-channels with orthogonal subcarriers, and transmitting a  $M$ -ary quadrature amplitude modulation (MQAM) symbol on each of the subcarriers. Even in the presence of severe multipath, each subchannel is affected by flat-fading, which can be easily equalized. A guard time interval between symbols prevents inter-symbol interference. Additionally, OFDM modulation supports high peak data rates and non-line-of-sight applications [1].

As OFDM symbols are transmitted through a channel, they undergo distortion due to noise and multipath effects. To counteract the effects of channel distortion, an estimate of channel characteristics must be calculated. In most standards, this is done using preambles and pilot signals, resulting in a loss of data rate. Additionally, most standards use a cyclic prefix (CP) during their guard intervals, which results in a loss of power efficiency since this information is disregarded at the receiver.

A method of blind channel equalization that can be applied to OFDM has been proposed by P. P. Viadyanathan et al [2], [3]. This method uses a zero prefix (ZP) vice a CP, the reason being that the transmitted ZP constrains the received signal to a subspace from which the channel information is extracted. This increases both data throughput and power efficiency.

The method of blind equalization proposed in [2] is investigated in this thesis. The method is implemented in MATLAB with both off-line and real-time channel

estimation investigated. Although the method in [2] uses a ZP, we show that it can be extended to the most traditional CP based OFDM by some simple preprocessing of the received data.

The method proposed in [2] was implemented as a recursive algorithm using a least mean squares (LMS) adaptive estimation method. However, it has been found that it is very sensitive to the SNR of the received signal.

In this research, the approach in [2] has been re-derived and a third, alternative adaptive algorithm implemented. This method also uses a LMS adaptive estimation method; however, it is shown to be more robust. Both adaptive methods can be fine-tuned by properly setting their step size. This thesis investigated two LMS step sizes, determined empirically.

The performance of these algorithms under different conditions is also compared. The first simulation was a comparison of their performance in a channel with additive white Gaussian noise (AWGN). The third method of channel estimation with the larger of the two step sizes performed the best in high signal-to-noise ratio (SNR) conditions (around 30dB). The second simulation used a non-stationary channel without AWGN modeled as a simple random walk. In this case, the original method of channel estimation and the alternative adaptive method had similar results, although the alternative adaptive method with the larger step size performed slightly better at channel rates of change of 0.08 percent of the total channel power.

Since both adaptive methods require an estimate of the channel as an initial condition, the final test run on the two algorithms was a comparison of how long it would take the channel estimate to converge with an inaccurate initial channel estimate. In this case, the more robust alternative adaptive method with the larger step size once again outperformed the initial adaptive method.

Finally, this thesis investigates a method of estimating data lost in nulls caused by deep fading in the wireless channel, due to multipath. The algorithm was implemented in MATLAB, and compared to a normal OFDM receiver that does not conduct null

estimation. The proposed null-estimating algorithm has similar error rates to the original receiver for SNRs less than approximately 21 dB but then significantly outperforms it and recovers the data lost in nulls for larger SNRs.

- [1] J. G. Andrews et al., *Fundamentals of WiMAX*. San Francisco, CA: Prentice Hall, 2007.
- [2] P. P. Vaidyanathan and B. Vrcelj, “A frequency domain approach for blind identification with filter bank precoders,” in *Proc. 2004 Int. Symp. Circuits and Systems*, pp. III- 349–52, 2004.
- [3] P. P. Vaidyanathan and B. Su, “Remarks on certain new methods for blind identification of FIR channels,” in *Conf. Rec. 38<sup>th</sup> Asilomar Conf. Signals, Systems and Computers*, Asilomar, CA, pp. I- 832–836, 2004.

THIS PAGE INTENTIONALLY LEFT BLANK

## **ACKNOWLEDGMENTS**

I would like to thank Professors Roberto Cristi and Frank Kragh for their help in completing this thesis. I would also like to thank my wife, who helped me with the finishing touches.

THIS PAGE INTENTIONALLY LEFT BLANK

# I. INTRODUCTION

## A. BACKGROUND

Orthogonal frequency-division multiplexing (OFDM) modulation has become the modulation method of choice for wireless broadband communications. It is currently in use in numerous standards, including IEEE standards 802.11 and 802.16, and military wireless communications such as the Wideband Networking Waveform of the Joint Tactical Radio System. The reason for its proliferation comes from the advantages that it has over other methods of modulation. The main advantage is that the technique allows high data rate transmissions to be sent over channels that experience multipath fading.

One of the challenges of this modulation technique is that it requires knowledge of the multipath channel to perform equalization. How to acquire knowledge of the channel using blind equalization is examined in this thesis. This is significant since it increases the throughput of the channel by reducing (or eliminating) the need for pilot signals normally embedded in the OFDM symbol.

## B. OBJECTIVES AND METHODOLOGY

The goal of this thesis was to further investigate the method of blind channel equalization proposed by P. P. Vaidyanathan, et al. [1]. Once the method had been implemented in code, a binary or quadrature phase-shift keyed (BPSK or QPSK respectively) signal was sent through either a channel with additive white Gaussian noise (AWGN) or a non-stationary channel modeled by a simple random walk.

Once this was completed, the method was implemented using a least mean squares (LMS) estimation technique. This method was also tested using BPSK and QPSK signals through either a channel with AWGN or a non-stationary channel. It was also tested using an inaccurate initial channel estimate to determine how long the channel estimate would take to converge to the correct channel.



Additionally, a secondary LMS method was implemented to overcome ill-conditioning issues with the initial LMS method. This was tested in the same manner as the first LMS method.

Finally, this paper shows an additional advantage of the secondary LMS method; namely, that this technique allows for the recovery of information sent through deep fading channels.

### **C. BENEFITS OF STUDY**

Demand for data, specifically multimedia content, continues to increase in a nearly exponential manner [2]. This has led to an increased demand on mobile broadband technologies, including 4G phone technology and WiMAX [3]. Both these emerging technologies use OFDM modulation. By reducing or eliminating pilot signals in the OFDM symbol, the amount of data throughput is increased. Additionally, if a zero prefix (ZP) is used instead of a cyclic prefix (CP), it saves power at the transmitting station, whether it is a mobile or base station [3].

### **D. ORGANIZATION**

This thesis is organized into six chapters. Chapter II is a background discussion of OFDM modulation, and examples of its use in current standards are provided. Chapter III contains an in-depth discussion of the blind equalization method proposed in [1]. An adaptive estimation method based on the discrete Fourier transform (DFT) is proposed in Chapter IV. Simulation results from the adaptive method are compared with simulation results from the original in Chapter IV. A method of recovering the information lost in deep fading channels is discussed in Chapter V, and the results of the implementation of this method are presented. Finally, a summary of the work in this thesis, significant results, and recommendations for future work are given in Chapter VI.

## II. OVERVIEW OF OFDM

Orthogonal frequency-division multiplexing is a method of multicarrier modulation used in a variety of standards for both wired and wireless communications. A brief overview of OFDM modulation and its use in IEEE standards 802.11a, 802.11g, and 802.11n is provided in this chapter.

The principle behind OFDM is the idea that a wideband frequency channel can be divided into subchannels with narrower bands on which data can be transmitted. Orthogonality of the subcarriers, in a sense specified later, prevents interference between the subbands. This technique is particularly useful when transmitting through frequency-selective channels arising from environments that have severe multipath, and it allows simple channel equalization at the receiver [4].

In OFDM, the data is transmitted in blocks via a sequence of OFDM symbols, separated by a guard time interval to prevent inter-symbol interference (ISI). This is guaranteed by choosing the guard time between OFDM symbols to be larger than the maximum channel time spread [4].

A key issue addressed in this thesis is what is best to transmit during the guard time. In the most common implementations of OFDM, such as in IEEE Standards 802.11, 802.16, and others, the CP is used, which is a cyclic repetition transmitted as the guard interval. A consequence of choosing to transmit the CP is that it becomes very easy to demodulate the signal in the frequency domain, since linear convolution becomes circular convolution where the fast Fourier transform (FFT) plays a dominant role.

In a number of papers [1][5], it is shown that a ZP, obtained by transmitting all zeros during the guard interval, is an attractive alternative to a CP because it yields sufficient information to perform blind equalization. In other words, in principle at least, with the ZP the channel can be estimated from the received data without the need of pilots and/or training signals. This is due to the fact that, with the addition of the transmitted zeros, the received signal is constrained on a subspace that yields the channel information, regardless of the transmitted data.

This research takes this issue even further. It shows that another advantage of using an OFDM symbol with ZP (rather than the standard CP) is the fact that by using a longer FFT at the receiver, subcarriers with low signal-to-noise ratio (SNR) due, for example, to deep fading, can still be reliably recovered using simple properties of the FFT. Of course, this comes with some added complexity but is still manageable with today's technology.

Interestingly, with some minor preprocessing, the ZP OFDM approach can be extended to the existing CP OFDM with the same advantages of blind equalization and robust recovery in deep fading channels.

### A. OFDM SYMBOL

In OFDM, the transmitted signal is defined as

$$s(t) = \text{Re} \left\{ e^{j2\pi F_c t} x(t) \right\} \quad (1)$$

where  $F_c$  is the carrier frequency, and the baseband complex signal is defined as

$$x(t) = \sum_{\substack{k=-\frac{N_F}{2} \\ k \neq 0}}^{\frac{N_F}{2}} c_k e^{j2\pi k \Delta F t} \quad 0 \leq t \leq T_{symbol} \quad (2)$$

where the coefficients  $c_k$  depend on the transmitted data and  $N_F$  is the number of subcarriers. The symbol length  $T_{symbol}$  is made of the data length  $T_b$  and the time guard length  $T_g$  as

$$T_{symbol} = T_b + T_g . \quad (3)$$

To ensure that the subcarriers are orthogonal to one another, the difference between subcarrier frequencies is chosen to be

$$\Delta F = \frac{1}{T_b} . \quad (4)$$

This results in the following integral, which defines the orthogonality of the subcarriers:

$$\frac{1}{T_b} \int_{t_0}^{t_0+T_b} e^{j2\pi F_k t} e^{-j2\pi F_l t} dt = \frac{1}{T_b} \int_{t_0}^{t_0+T_b} e^{j2\pi(k-l)\Delta F t} dt = \begin{cases} 1 & \text{if } k = l \\ 0 & \text{if } k \neq l \end{cases} . \quad (5)$$

If the channel is linear time-invariant (LTI), at least within the symbol duration, and the guard time  $T_g$  is greater than the channel time spread, the subcarriers are still orthogonal at the receiver and are given by

$$y(t) = \sum_k c_k H(F_k) e^{j2\pi F_k t} \quad T_g \leq t \leq T_{symbol}, \quad (6)$$

where  $H(F)$  is the frequency response of the channel [4].

The discrete time implementation is very straightforward. Let  $F_s$  be the sampling frequency,  $N$  be the number of data samples in each symbol, and  $\Delta F = 1/NT_s = F_s/N$  be the subcarrier spacing. Then (2) becomes

$$x(nT_s) = \frac{1}{N} \sum_{k=-\frac{N_F}{2}}^{\frac{N_F}{2}} c_k e^{j2\pi k \frac{\Delta F}{F_s}(n-L)} = \frac{1}{N} \sum_{k=-\frac{N_F}{2}}^{\frac{N_F}{2}} c_k e^{jk \frac{2\pi}{N}(n-L)} \quad n = 0, \dots, L + N - 1 \quad (7)$$

where the guard time is  $T_g = LT_s$  and the scale factor of  $1/N$  is immaterial but is included for later convenience. This result leads itself to using the inverse fast Fourier transform (IFFT) to complete the precoding necessary for OFDM:

$$x[n + L] = \frac{1}{N} \sum_{k=-\frac{N_F}{2}}^{\frac{N_F}{2}} c_k e^{jk \frac{2\pi}{N} n}. \quad (8)$$

If  $X[k] = c_k$  for positive subcarriers ( $k > 0$ ),  $X[N + k] = c_k$  for negative subcarriers ( $k < 0$ ), and  $X[k] = 0$  for  $k = 0$ , then (8) can be written in terms of the IFFT as

$$x[n + L] = \frac{1}{N} \sum_{k=0}^{N-1} X[k] e^{jk \frac{2\pi}{N} n} = \text{IFFT}\{X[k]\}. \quad (9)$$

From (2) and the subcarrier frequencies being multiples of  $\Delta F$  in (4), it is easy to see that the data transmitted during the guard interval is just a periodic repetition. In particular, the CP is comprised of the last  $L$  points of the  $\text{IFFT}\{X[k]\}$ .

The demodulation of the OFDM signal is based on the convolution of the channel impulse response and the signal:

$$\begin{aligned}
y[n] &= h[n] * x[n] \\
&= h[n] * \frac{1}{N} \sum_{k=0}^{N-1} X[k] e^{j\frac{2\pi}{N}kn} \\
&= \frac{1}{N} \sum_{k=0}^{N-1} H[k] X[k] e^{j\frac{2\pi}{N}kn} \\
&= \text{IFFT} \{ H[k] X[k] \}
\end{aligned} \tag{10}$$

Based on the results of (10), the following conclusion can be drawn:

$$\begin{aligned}
H[k] X[k] &= \text{FFT} \{ y[L], \dots, y[L+N-1] \} \\
\text{with } H[k] &= \text{FFT} \{ h[0], \dots, h[L-1], 0, \dots, 0 \} \quad k = 0, \dots, N-1
\end{aligned} \tag{11}$$

The block diagram of a simple OFDM communication system is shown in Figure 1.

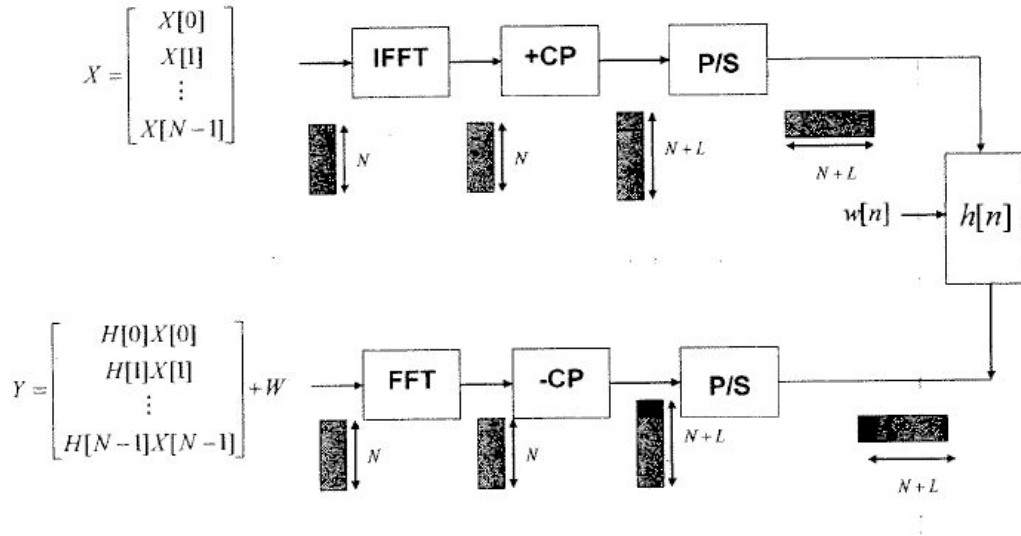


Figure 1. A block diagram of a simple OFDM communications system. From [4].

Since for the  $k$ -th subcarrier, the received signal is of the form

$$Y[k] = H[k]X[k] + W[k] \tag{12}$$

where  $W[k]$  is the FFT of  $w[n]$ , additive noise, the transmitted signal  $X[k]$  can be recovered using a Weiner Filter as

$$\hat{X}[k] = \frac{H^*[k]}{|H[k]|^2 + \sigma_w^2} Y[k] \quad (13)$$

if the channel frequency response is known.

There are some limitations to this approach of OFDM modulation. The CP does not contain useful data and is just overhead for the modulation technique. Additionally, the channel imposes some constraints on the length of the data interval such that it must be larger than the maximum channel time spread to minimize overhead and must be much smaller than then period associated with the Doppler spread to maintain the LTI channel assumption [4].

The advantages of OFDM are that it is effective in multipath environments, it is efficient in implementation, and the data rate can be optimized based on channel conditions and noise characteristics. The disadvantages are that it is sensitive to time and frequency synchronization, and data can be lost when there are spectral nulls in the channel frequency response [4].

## **B. OFDM IN STANDARDS**

### **1. IEEE Standard 802.11a**

IEEE Standard 802.11a, which describes the high-speed physical layer in the 5GHz band, uses OFDM to transmit data over wireless local area networks (LANs) [6]. The standard uses 52 sub-carriers, four of which carry the pilot signal and 48 that carry the data. The  $\Delta F$  is set at 0.3125 MHz, with the guard interval  $0.8 \mu s$  long and the data interval  $3.2 \mu s$  long. The mapping of the 52 sub-carriers to the time domain outputs can be seen in Figure 2.

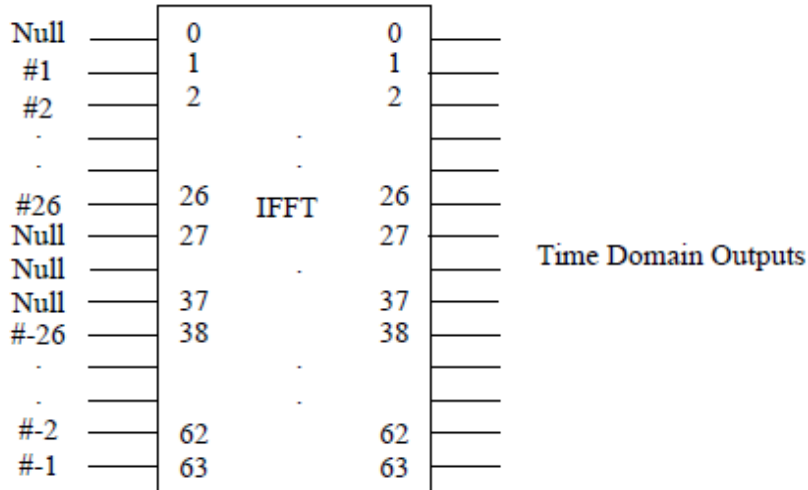


Figure 2. Mapping of IFFT inputs to time-domain outputs for 802.11a. From [7].

## 2. IEEE Standard 802.11g

IEEE Standard 802.11g, is a modification of the 802.11 standards for the 2.4-GHz band to include OFDM modulation. The inputs to the IFFT retain the same structure as those in 802.11a but with a lower carrier frequency

## 3. IEEE Standard 802.11n

IEEE Standard 802.11n uses OFDM modulation in a multiple-input multiple-output (MIMO) scheme to attain higher throughput and more robustness to multipath and noise for both the 2.4- and 5-GHz bands [8]. It provides up to four spatial streams of OFDM modulated data to achieve a maximum data rate of 600 Mbps.

## 4. Other Standards

OFDM modulation is also used in various other applications. WiMAX is based on IEEE Standard 802.16, an OFDM based system. Other standards that use OFDM modulation include power-line communications, various digital television and radio standards, and the Wideband Networking Waveform of the Joint Tactical Radio System.

These applications of OFDM use pilot signals and training symbols to conduct channel equalization. In the next chapter, we see how channel equalization can be conducted without the use of these methods.



THIS PAGE INTENTIONALLY LEFT BLANK

### III. BLIND CHANNEL ESTIMATION IN OFDM WITH ZERO PREFIX

A class of blind equalization algorithms has been presented by P. P. Vidyathan et al. in a number of papers [1], [5], which can easily be extended to OFDM with ZP. Their argument is presented in this chapter. An alternative derivation of their results is at the basis of further properties of this algorithm, as is presented in Chapters IV and V.

#### A. BLIND EQUALIZATION USING A ZERO PREFIX

In the method described in [1], the CP used in the standards discussed in Chapter II is replaced with the use of a ZP. Instead of filling the guard interval with data from the end of the data block or the last  $L$  samples of the data block, the data is zero-padded with  $L$  zeros during the guard interval. As long as the guard interval is still longer than the maximum time spread of the channel, there is no ISI.

In ZP OFDM the data is transmitted as a sequence of discrete time OFDM symbols  $x[0], x[1], \dots, x[n], \dots$ , defined as

$$\underline{x}[n] = \begin{bmatrix} x_0[n] \\ x_1[n] \\ \vdots \\ x_{M-1}[n] \\ 0 \\ \vdots \\ 0 \end{bmatrix} \in \mathbb{C}^{P \times 1} \quad (14)$$

where  $M$  is the length of the FFT and IFFT, and  $P = M + L$  is the overall length of the OFDM symbol, including the ZP. Then each input block is in a subspace of  $\mathbb{C}^{P \times 1}$ . If there is no noise, the received signal

$$\underline{y}[n] = \begin{bmatrix} y_0[n] \\ y_1[n] \\ \vdots \\ y_{P-1}[n] \end{bmatrix} \in \mathbb{C}^{P \times 1} \quad (15)$$

is also in a subspace of  $\mathbb{C}^{Px1}$ . With this in mind, it is possible to show that the channel impulse response  $c[l]$  can be estimated from the subspace of  $\underline{y}[n]$  without knowledge of the input signal  $\underline{x}[n]$ .

## B. CHANNEL ESTIMATION

The general principles behind the method proposed in [1] are discussed in this section. Let the  $n$ -th data block be defined as

$$\underline{s}[n] = \begin{bmatrix} s_0[n] \\ \vdots \\ s_{M-1}[n] \end{bmatrix}. \quad (16)$$

The data block is then encoded with a matrix  $R_1 \in \mathbb{C}^{M \times M}$  which in the cases of OFDM modulation is associated with the IFFT.

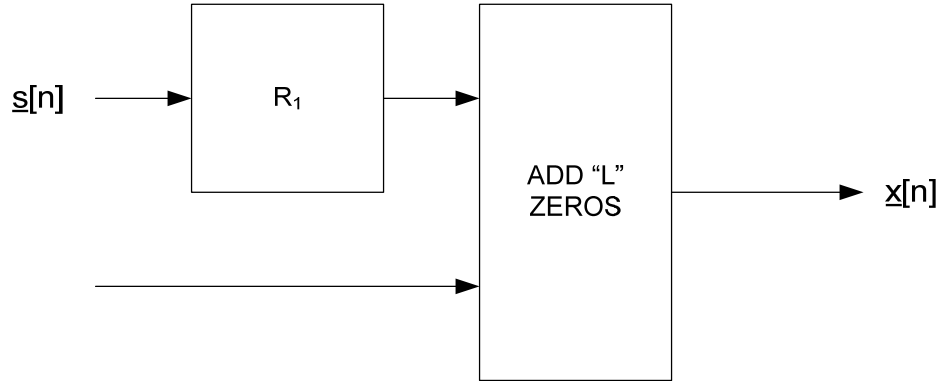


Figure 3. The signal  $\underline{s}[n]$  is encoded with the  $R_1$  matrix, then  $L$  zeros are appended. After [7].

After precoding, the transmitted blocks  $\underline{x}[n]$  are defined as:

$$\underline{x}[n] = \begin{bmatrix} R_1 \\ 0 \end{bmatrix} \underline{s}[n]. \quad (17)$$

Notice that  $\underline{x}[n]$  can be written as

$$\underline{x}[n] = [x_0[n], x_1[n], \dots, x_{M-1}[n], 0, \dots, 0]^T, \quad (18)$$

with the zeros indicating the zero prefix. Although the appended zeros really represent a suffix, for clarity of discussion, they will continue to be referred to as the zero prefix.

In the section that follows, it can be seen that the received signal has a particular structure from which the channel's characteristics can be extracted without knowledge of the transmitted data.

### 1. Received OFDM Symbol

The output from the channel in the time domain is the convolution of the impulse response of the channel with  $x(t)$ . Since there is no ISI due to the ZP, each block can be examined separately, and the received signal for the  $n$ -th block becomes

$$y_l[n] = \sum_{k=0}^{L-1} c[k]x_{l-k}[n] \quad l = 0, 1, \dots, P-1 \quad (19)$$

with  $c[k]$ ,  $k = 0, \dots, L-1$ , the impulse response of the channel. Then it is easy to verify that

$$\begin{bmatrix} y_0[n] \\ y_1[n] \\ \vdots \\ y_{p-1}[n] \end{bmatrix} = \begin{bmatrix} c[0] & 0 & \dots & 0 \\ c[1] & c[0] & \dots & \vdots \\ \vdots & c[1] & \dots & \vdots \\ c[L-1] & \vdots & \dots & 0 \\ 0 & c[L-1] & \dots & c[0] \\ \vdots & 0 & \dots & c[1] \\ \vdots & \vdots & \dots & \vdots \\ 0 & 0 & \dots & c[L-1] \end{bmatrix} \begin{bmatrix} x_0[n] \\ \vdots \\ x_{M-1}[n] \end{bmatrix} \quad (20)$$

which can be represented in matrix form as

$$\underline{y}[n] = A\underline{x}_d[n] = A\underline{R}_1\underline{s}[n] \quad (21)$$

with  $\underline{y}[n]$  a  $P \times 1$  vector,  $\underline{x}_d[n]$ , the data only version of  $\underline{x}[n]$ , a  $M \times 1$  vector, and  $A$  a  $P \times M$  matrix. The matrix  $A$  contains the information of the channel and it has an interesting property. Given any complex variable  $z$ , it can be shown that

$$\begin{bmatrix} 1, & z^{-1}, & z^{-2}, & \dots, & z^{-(P-1)} \end{bmatrix} \begin{bmatrix} c[0] & 0 & \dots & 0 \\ c[1] & c[0] & \dots & \vdots \\ \vdots & c[1] & \dots & \vdots \\ c[L-1] & \vdots & \dots & 0 \\ 0 & c[L-1] & \dots & c[0] \\ \vdots & 0 & \dots & c[1] \\ \vdots & \vdots & \dots & \vdots \\ 0 & 0 & \dots & c[L-1] \end{bmatrix} = \begin{bmatrix} C(z), & z^{-1}C(z), & z^{-2}C(z), & \dots, & z^{-(M-1)}C(z) \end{bmatrix}, \quad (22)$$

with  $C(z)$ , the transfer function of the channel, defined as

$$C(z) = \sum_{l=0}^{L-1} c[l]z^{-l} = \mathbb{Z}\{c[l]\}. \quad (23)$$

The right hand side of (22) becomes

$$C(z) \begin{bmatrix} 1, & z^{-1}, & \dots, & z^{-(M-1)} \end{bmatrix}. \quad (24)$$

Using the results above, we see how the transmitted data  $\underline{s}[n]$  can be recovered from the received data  $\underline{y}[n]$  assuming that there is no noise. Let

$$\hat{\underline{s}}[n] = E \underline{y}[n], \quad E \in \mathbb{C}^{M \times P}, \quad (25)$$

with  $E$ , an arbitrary  $M \times P$  matrix to be determined later. Substitute (21) into (25), and the following equation results:

$$\begin{aligned} \hat{\underline{s}}[n] &= E A R_1 \underline{s}[n] \\ &= \begin{bmatrix} E \end{bmatrix} \begin{bmatrix} A \\ R_1 \end{bmatrix} \underline{s}[n]. \end{aligned} \quad (26)$$

Now, let  $E$  be of the form

$$E = \begin{bmatrix} \underline{e}_0^T \\ \vdots \\ \underline{e}_{M-1}^T \end{bmatrix}, \quad (27)$$

where  $\underline{e}_k^T$  is defined as

$$\underline{e}_k^T = \frac{1}{C(\rho_k)} \begin{bmatrix} 1, & \rho_k^{-1}, & \rho_k^{-2}, & \dots, & \rho_k^{-(P-1)} \end{bmatrix} \quad k = 0, \dots, M-1. \quad (28)$$

$\rho_i \neq \rho_j$

If a new matrix is defined as

$$\Lambda_M = \begin{bmatrix} C(\rho_0) & 0 & \cdots & 0 \\ 0 & \ddots & \ddots & \vdots \\ \vdots & \ddots & \ddots & 0 \\ 0 & \cdots & 0 & C(\rho_{M-1}) \end{bmatrix}, \quad (29)$$

then it can be seen that

$$\begin{aligned} EA &= \Lambda_M^{-1} \begin{bmatrix} 1 & \rho_0^{-1} & \cdots & \rho_0^{-(P-1)} \\ \vdots & \vdots & \vdots & \vdots \\ 1 & \rho_{M-1}^{-1} & \cdots & \rho_{M-1}^{-(P-1)} \end{bmatrix} A \\ &= \Lambda_M^{-1} \Lambda_M \begin{bmatrix} 1 & \rho_0^{-1} & \cdots & \rho_0^{-(P-1)} \\ \vdots & \vdots & \vdots & \vdots \\ 1 & \rho_{M-1}^{-1} & \cdots & \rho_{M-1}^{-(P-1)} \end{bmatrix}. \\ &= V_{M \times M} \end{aligned} \quad (30)$$

Substituting the results of (30) into (26), we reach the conclusion that

$$\widehat{\underline{s}}[n] = V_{M \times M} R_1 \underline{s}[n]. \quad (31)$$

The transmitter-receiver structure in (25)-(31) is more general than standard OFDM. It can be easily seen that the choice

$$\rho_k = e^{jk \frac{2\pi}{M}} \quad k = 0, \dots, M-1 \quad (32)$$

will yield the standard OFDM. In this case, the operation can be done using FFTs if the  $R_1$  matrix is chosen carefully; namely,

$$R_1 = V_{M \times M}^{-1}. \quad (33)$$

## 2. Channel Estimation from a Block of Received Data

If the received vectors are organized column-wise into a matrix and the number of received vectors is much larger than the length of the OFDM symbol such that

$$Y = [\underline{y}[0], \underline{y}[1], \dots, \underline{y}[J-1]] \quad J \gg P, \quad (34)$$

then it follows that  $Y$  is a  $P \times J$  matrix of the form

$$Y = AR_1 [\underline{s}[0], \underline{s}[1], \dots, \underline{s}[J]]. \quad (35)$$

From (35) it can be seen that  $Y$  is not a full rank matrix since the columns of  $A$  in (22) span an  $M$ -dimensional subspace of  $\mathbb{C}^P$ . Therefore, a matrix  $V$  exists such that

$$VY = 0 \quad (36)$$

Since the matrix of transmitted data is most likely full rank, the matrix  $V$  also satisfies  $VA = 0$  or, more explicitly,

$$V \begin{bmatrix} c[0] & 0 & \cdots & 0 \\ c[1] & c[0] & \cdots & \vdots \\ \vdots & c[1] & \cdots & \vdots \\ c[L-1] & \vdots & \cdots & 0 \\ 0 & c[L-1] & \cdots & c[0] \\ \vdots & 0 & \cdots & c[1] \\ \vdots & \vdots & \cdots & \vdots \\ 0 & 0 & \cdots & c[L-1] \end{bmatrix} = 0. \quad (37)$$

The matrix  $V$ , which can be computed from the null space of  $Y$ , contains the information of the channel, as can be seen next.

To extract the channel information from the  $V$  matrix, several more steps are required. Let  $G$  be a  $P \times P$  matrix, featuring a structure similar to  $E$  in (27),

$$G = \begin{bmatrix} \underline{e}_0^T \\ \underline{e}_1^T \\ \vdots \\ \underline{e}_{M-1}^T \\ \underline{e}_M^T \\ \vdots \\ \underline{e}_{P-1}^T \end{bmatrix} \quad (38)$$

where

$$\begin{aligned} \underline{e}_k^T &= [1, \rho_k^{-1}, \rho_k^{-2}, \dots, \rho_k^{-(P-1)}] \\ k &= 0, \dots, P-1 \\ \rho_i &\neq \rho_j \end{aligned} \quad (39)$$

Although this is more general, OFDM would correspond to the choice  $\rho_k = e^{jw_k}$  for some  $w_k$ . Now, let the  $G$  matrix be used for post-processing of the received signal. For the illustration of this post-processing, a new  $\underline{y}'[n]$  is defined:

$$\underline{y}'[n] = GAR_1 \underline{s}[n]. \quad (40)$$

Notice that (38) and (40) yield a similar receiver to the one defined by (25) and (27), only with an extended set of frequencies at the demodulator.

Now, substituting (38) for  $G$  into (40), we obtain

$$\underline{y}'[n] = \begin{bmatrix} \underline{e}_0^T \\ \underline{e}_1^T \\ \vdots \\ \underline{e}_{M-1}^T \\ \underline{e}_M^T \\ \vdots \\ \underline{e}_{P-1}^T \end{bmatrix} AR_1 \underline{s}[n]. \quad (41)$$

If  $V_{L \times M}$  is defined as the first  $M$  columns of  $G$ ,  $\Lambda_M$  is defined in (29) and  $\Lambda_L$  is defined

$$\Lambda_L = \begin{bmatrix} C(\rho_M) & 0 & \cdots & 0 \\ 0 & \ddots & \ddots & \vdots \\ \vdots & \ddots & \ddots & 0 \\ 0 & \cdots & 0 & C(\rho_{P-1}) \end{bmatrix}, \quad (42)$$

then (41) can be written as

$$\underline{y}'[n] = \begin{bmatrix} \Lambda_M & 0 \\ 0 & \Lambda_L \end{bmatrix} \begin{bmatrix} V_{M \times M} \\ V_{L \times M} \end{bmatrix} R_1 \underline{s}[n]. \quad (43)$$

Since  $R_1$  was chosen as  $V_{M \times M}^{-1}$ , (43) can now be rewritten as

$$\underline{y}'[n] = \begin{bmatrix} \Lambda_M & 0 \\ 0 & \Lambda_L \end{bmatrix} \begin{bmatrix} I \\ B \end{bmatrix} \underline{s}[n], \quad (44)$$

where

$$B = V_{L \times M} R_1. \quad (45)$$

Recall that  $V$  is an  $M \times P$  complex matrix such that the product of  $V$  and the  $Y$  matrix defined in (34) is equal to zero. It follows that

$$V \underline{y}[n] = 0 \quad \forall n. \quad (46)$$

This implies



$$V \begin{bmatrix} \Lambda_M & 0 \\ 0 & \Lambda_L \end{bmatrix} \begin{bmatrix} I \\ B \end{bmatrix} = 0 \quad (47)$$

or, by properly partitioning  $V$ ,

$$\begin{bmatrix} V_1 & V_2 \end{bmatrix} \begin{bmatrix} \Lambda_M \\ \Lambda_L B \end{bmatrix} = 0 \quad (48)$$

To satisfy (48), the  $V$  matrix can be chosen

$$V = \begin{bmatrix} V_1 & V_2 \end{bmatrix} = \begin{bmatrix} \Lambda_L B \Lambda_M^{-1} & -I \end{bmatrix}, \quad (49)$$

where  $I$  is an  $L \times L$  identity matrix. This  $V$  matrix must also be equal to zero when multiplied with the  $Y$  matrix, meaning that

$$\begin{bmatrix} \Lambda_L B \Lambda_M^{-1} & -I \end{bmatrix} \begin{bmatrix} Y_0 \\ Y_1 \end{bmatrix} = 0, \quad (50)$$

where  $Y_0$  is a matrix of the first  $M$  rows of  $Y$ , and  $Y_1$  is a matrix of the last  $L$  rows of  $Y$ . From (50) it is easy to see that

$$\Lambda_L B \Lambda_M^{-1} Y_0 = Y_1. \quad (51)$$

Using linear algebra on (51), we get

$$\begin{aligned} \Lambda_L B \Lambda_M^{-1} Y_0 &= Y_1, \\ \Lambda_L B \Lambda_M^{-1} Y_0 Y_0^* &= Y_1 Y_0^*, \\ \Lambda_L B \Lambda_M^{-1} &= Y_1 Y_0^* (Y_0 Y_0^*)^{-1}, \\ \Lambda_L B &= Y_1 Y_0^* (Y_0 Y_0^*)^{-1} \Lambda_M. \end{aligned} \quad (52)$$

Let

$$Z_0 = Y_1 Y_0^* (Y_0 Y_0^*)^{-1} \quad (53)$$

where

$$Z_0 \in \mathbb{C}^{L \times M}. \quad (54)$$

Equation (52) then becomes

$$\Lambda_L B = Z_0 \Lambda_M. \quad (55)$$

If the structure of (55) is examined more closely and the  $k$ -th row of both sides are taken,

$$\begin{bmatrix} \ddots & & \\ & C(\rho_{M+k}) & \\ & \ddots & \end{bmatrix} \begin{bmatrix} b_{k,0} & \cdots & b_{k,M-1} \end{bmatrix} = \begin{bmatrix} z_{k,0} & \cdots & z_{k,M-1} \end{bmatrix} \begin{bmatrix} C(\rho_0) & & 0 \\ & \ddots & \\ 0 & & C(\rho_{M-1}) \end{bmatrix}, \quad (56)$$

then \

$$C(\rho_{M+k}) \begin{bmatrix} b_{k,0} & \cdots & b_{k,M-1} \end{bmatrix} = \begin{bmatrix} z_{k,0} C(\rho_0), & z_{k,1} C(\rho_1), & \cdots, & z_{k,M-1} C(\rho_{M-1}), \end{bmatrix}. \quad (57)$$

With one last manipulation, the frequency response for each of the frequencies associated with the  $M$  point IFFT is

$$\begin{aligned} C(\rho_l) &= \frac{1}{C(\rho_{M+k})} \frac{b_{k,l}}{z_{k,l}} \\ l &= 0, 1, \dots, M-1 \\ k &= 0, 1, \dots, L-1 \end{aligned} \quad (58)$$

The  $C(\rho_{M+k})$  term is a constant associated with all frequencies of the channel response. Additionally, for robustness in the presence of noise, the channel response can be averaged over the  $k$  rows of the matrix.

In conclusion, the channel frequency response, apart from a scaling factor, can be computed from a block of received OFDM symbols, as in (34), as follows:

Step 1: Let  $V_{L \times M}$ ,  $V_{M \times M}$  be the first  $L \times M$  and the last  $L \times L$  blocks of  $G$  in Equation (38).

Step 2: Compute  $B = V_{L \times M} R_1$ .

Step 3: Let  $Y_0$  and  $Y_1$  be the first  $M$  rows and last  $L$  rows of  $Y$ , respectively.

Step 4: Compute  $Z_0 = Y_1 Y_0^* (Y_0 Y_0^*)^{-1}$ .

Step 5: Call  $z_k$  and  $b_k$  any row  $k$  of  $Z_0$  and  $B$ .

Step 6:  $C(\rho_0)$ ,  $C(\rho_1)$ ,  $\dots$ ,  $C(\rho_{M-1})$  is proportional to ratio of rows  $z_k$  and  $b_k$ .

The channel frequency response was calculated using a MATLAB program that implemented the above method. The next chapter discusses the adaptive method used for real-time processing of an OFDM signal.

THIS PAGE INTENTIONALLY LEFT BLANK

## IV. RECURSIVE IMPLEMENTATION

### A. OFDM WITH CYCLIC PREFIX AND OFDM WITH ZERO PREFIX

The blind channel equalization algorithm presented in Chapter III is not recursive, and a large number of received OFDM symbols are required to compute the channel estimate. In this chapter, a recursive method of computing the channel estimate for every block received using an LMS estimator is explained in detail. For the purposes of this portion of the thesis, a received signal similar in structure to that used by IEEE 802.11a is used. In this standard, the length of the IFFT  $M$  is 64 samples, and the length  $L$  of the cyclic prefix is 16, for an overall OFDM symbol length  $P$  of 80 samples [6].

The method of blind equalization described in Chapter III required a ZP. In this chapter, we will see that the CP OFDM symbol used in all standards can be reframed as a ZP OFDM symbol by simple preprocessing at the receiver.

To achieve this goal, a standard CP OFDM signal,  $y_{CP}[n]$ , can be made into a ZP OFDM signal by subtracting a delayed version of the signal to get

$$y_{ZP}[n] = y_{CP}[n] - y_{CP}[n - M]. \quad (59)$$

As shown in Figure 4, it is easy to see that the CP terms cancel since the data in the CP is the same as the data at the end of the OFDM symbol. To recover the old symbols, the new OFDM symbol and the phase shifted old symbol are simply added.

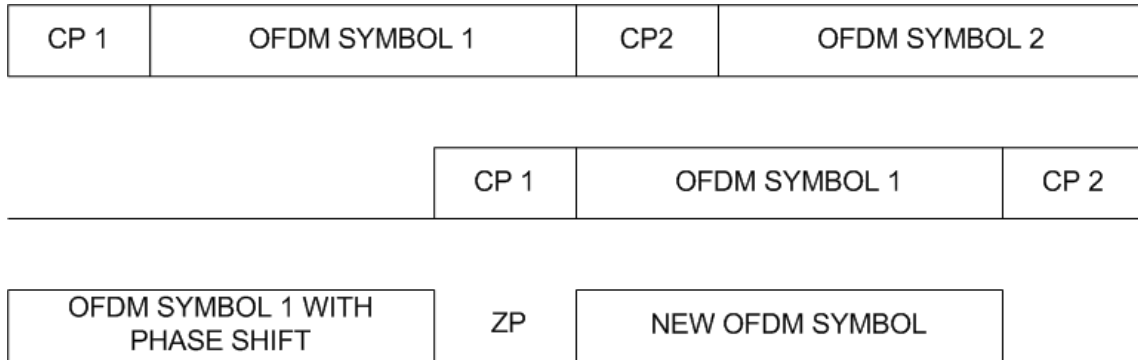


Figure 4. A delay of  $M$  points results in a phase shift of the first OFDM symbol with a ZP and new symbols subsequent to that.

Now the channel can be estimated using the algorithm discussed in the previous chapter and applied to the received OFDM symbol. The rest of this section describes the LMS filter method used as if a zero prefix OFDM symbol had been transmitted vice the CP OFDM symbol that was actually simulated.

Initially, an LMS estimator was derived directly from the off-line method described in Chapter III. This method is not robust, and the theory behind it is not presented in this thesis; however, some of the simulation results have been included for comparison purposes. In what follows we present a different approach to blind equalization for ZP OFDM, discussed in [9], which is more suitable to recursive implementation.

## B. PROPOSED APPROACH

In this section, a different approach to blind equalization of ZP OFDM is investigated based on standard properties of the DFT. The results of this section are based on [9].

The purpose of this approach is an improved estimation method that can be computed recursively with an LMS. The resulting method is shown to be effective in cases where the channel is initially poorly estimated or slowly changing with time. It also had an added benefit that is discussed in the next section of this chapter.

In order to introduce this approach, define a vector  $x$  of length  $2M$  such that

$$x[n] = 0, \text{ for } n = M, \dots, 2M - 1 \quad (60)$$

and a second vector  $w$  of the same length  $2M$  of the form

$$w[n] = \begin{cases} 0 & \text{if } 0 \leq n \leq M - 1 \\ 1 & \text{if } M \leq n \leq 2M - 1 \end{cases} \quad (61)$$

Clearly, no matter what  $x[n], n = 0, \dots, M - 1$  is, we have

$$x[n]w[n] = 0 \text{ for all } n = 0, \dots, 2M - 1. \quad (62)$$

Since multiplication of two finite length sequences corresponds to the circular convolution of the respective DFTs, we can write (62) in terms of  $W[k] = DFT\{w[n]\}$  and  $X[k] = DFT\{x[n]\}$ .

The DFT of the  $w$  vector is defined as

$$W[k] = \sum_{n=M}^{2M-1} e^{-j\frac{2\pi}{2M}kn}, \quad (63)$$

which is a geometric series. If  $l = n - M \Rightarrow n = l + M$ , then (63) can be rewritten as

$$W[k] = \begin{cases} \sum_{l=0}^{N-1} e^{-j\frac{2\pi}{2N}k(l+M)} = (-1)^k \frac{1 - (-1)^k}{1 - e^{-j\frac{\pi}{N}k}}, & \text{for } k = 1, \dots, 2M - 1 \\ M, & \text{for } k = 0 \end{cases}. \quad (64)$$

It is easy to see that  $W[k] = 0$  when  $k$  is even, and in particular

$$W[k] = \begin{cases} \frac{-2}{1 - e^{-j\frac{\pi}{N}k}} & \text{if } k \text{ odd} \\ 0 & \text{if } k \neq 0, \text{ even.} \\ M & \text{if } k = 0 \end{cases}. \quad (65)$$

Now, circularly convolve the DFTs of the two vectors  $x$  and  $w$  to get

$$\sum_{l=0}^{M-1} X[l]W[k-l] = 0, \quad (66)$$

where the shifted represented by  $k-l$  is a circular shift. If  $k$  is chosen to be any odd frequency, it can be shown that  $W[k-l]$  is not equal to zero only when  $k=l$  or  $l$  is even.

Using this conclusion, we see that when  $k$  is odd (66) becomes

$$\sum_{\substack{l=0 \\ l \text{ even}}}^{M-1} X[l]W[k-l] + X[k]W[0] = 0. \quad (67)$$

If the value for  $W[0]$  is substituted into (67) and the equation is rearranged, then

$$MX[k] = - \sum_{\substack{l=0 \\ l \text{ even}}}^{M-1} W[k-l]X[l]. \quad (68)$$

The relationship between the DFT of the transmitted signal and the DFT of the received signal is just the inverse of the channel frequency response; that is,

$$X[k] = \frac{Y[k]}{C[k]}. \quad (69)$$

For any odd value of  $k$ , (69) can then be substituted into (68) to get

$$MY[k]\frac{1}{C[k]} = - \left( \sum_{\substack{l=0 \\ l \text{ even}}}^{M-1} W[k-l]Y[l]\frac{1}{C[l]} \right). \quad (70)$$

If (70) is further deconstructed, with the  $l$  values associated with the data on the left-hand side, the  $l$  values associated with the pilots on the right-hand side, and an arbitrary odd value of  $k$ , then

$$\sum_{\substack{l=0 \\ l \text{ even}}}^{M-1} W[k-l]Y[l]\frac{1}{C[l]} + MY[k]\frac{1}{C[k]} = - \left( \sum_{\substack{l=0 \\ l \text{ even}}}^{M-1} W[k-l]X_{pilots}[l] \right). \quad (71)$$

With a few terms further defined, (71) lends itself to an LMS-type implementation; that is,

$$\begin{aligned} \underline{\phi}_{k,n}^T &= [W[k]Y[0], W[(k-2)]Y[2], \dots, MY[k]] \\ \underline{\theta} &= \left[ \frac{1}{C[0]}, \frac{1}{C[2]}, \dots, \frac{1}{C[M-2]}, \frac{1}{C[k]} \right] \\ v_{k,n} &= - \left( \sum_{\substack{l=0 \\ l \text{ even}}}^{M-1} W[k-l]X_{pilots}[l] \right) \end{aligned} \quad (72)$$

Now, from [9], the LMS estimator can be written as

$$\underline{\theta}_{new} = \underline{\theta}_{old} + \mu \underline{\phi}_{k,n}^* \left( \underline{\theta}_{old}^T \underline{\phi}_{k,n} - v_{k,n} \right). \quad (73)$$

### C. SIMULATION RESULTS

Each of the methods of implementation for the blind estimation of the channel were run using 100 trials at each data point, regardless of the type of test being run. Additionally, the number of OFDM symbols transmitted was set at 10,000. Using IEEE Standard 802.11a format, we have 52 BPSK or QPSK symbols per OFDM symbol, for a total of 52 million symbols per data point.

The number of pilot signals was reduced from four pilot symbols per OFDM symbol to one pilot symbol per five OFDM symbols. The purpose of transmitting the pilot symbol was to determine the channel constant for all three methods of implementation. However, the number of pilot signals sent could be further reduced depending on channel conditions.

The values of  $\mu$ , the LMS algorithm step size, were determined experimentally to ensure convergence of the adaptive algorithm. For the initial LMS implementation the step size  $\mu$  was set to a small value ( $10^{-7}$ ), and for the second DFT-based LMS implementation,  $\mu$  was set to a larger value ( $3 \times 10^{-5}$ ). These values can be adjusted to ensure the algorithm converges or to adjust the speed at which the algorithm converges.

### **1. Performance in the Presence of Multipath and AWGN**

To test the performance of the proposed DFT-based adaptive channel estimation method and the adaptive method based on the theory discussed in Chapter III, the respective performances were compared using the initial off-line, or block, blind estimation method. All three methods were tested with AWGN. The tests were run with SNRs from zero to 50 dB. Algorithm performance was determined by calculating the symbol error rate (SER), in errors per symbol. The results for the DFT based adaptive algorithm with an LMS step size of  $\mu = 10^{-7}$  and the block method is shown in Figure 5. The channels are modeled as random complex channels with an impulse response of the same length as the guard interval ( $L=16$  in this case).



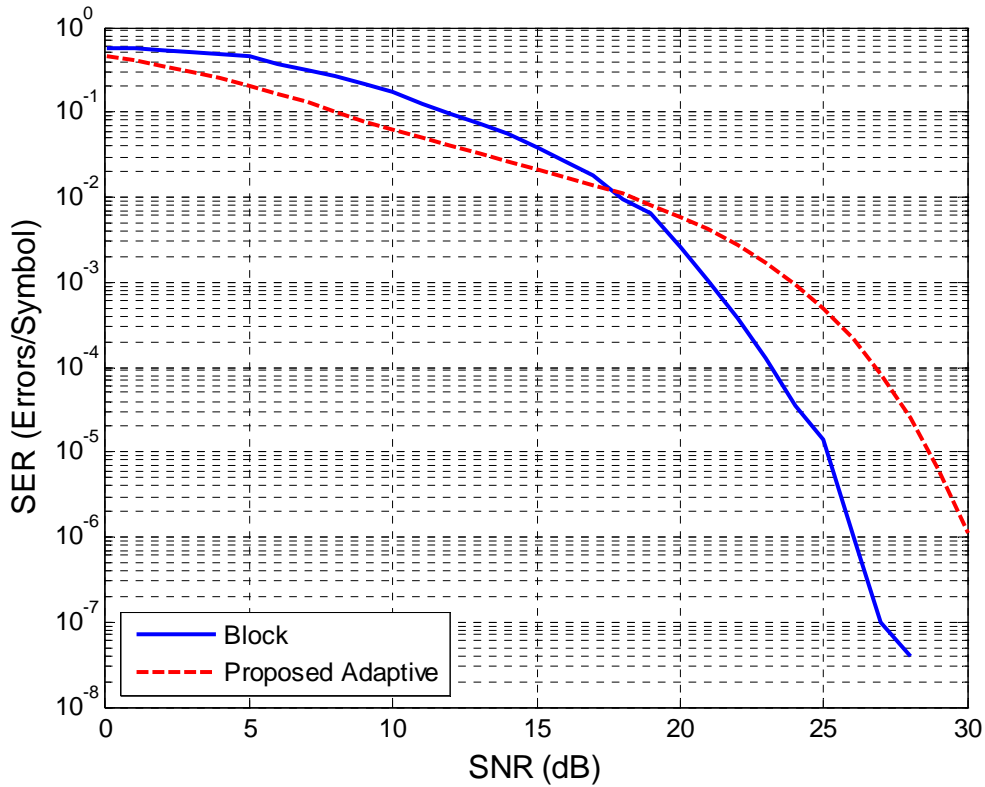


Figure 5. QPSK SER versus SNR with a step size of  $\mu = 10^{-7}$ .

For this thesis the SNR is defined as

$$SNR = \frac{E[s^2(t)]}{E[n^2(t)]}, \quad (74)$$

where  $s(t)$  is the signal and  $n(t)$  it the noise. It is related to  $E_b/N_o$  by a factor of  $B/R_b$ , where  $B$  is the bandwidth of the channel, and  $R_b$  is the data rate. For 802.11a QPSK, this factor is 0.692 [6].

It can be seen that, in this example, the proposed LMS method has better performance than the block processing approach presented in Chapter III for SNR less than 18 dB. At 5 dB, the proposed method out performs the block method by  $2.423 \times 10^{-1}$  errors/symbol, the maximum delta between the two methods. This is likely due to the fact that the block processing approach estimate is averaged over the  $k$  rows

of the matrix, as discussed in the previous chapter. Specifically, there are  $k$  estimates of the channel, one derived from every row of the matrix, and these estimates are averaged together before being applied to the received signal.

The results for the adaptive method discussed in Chapter III are not presented since the algorithm never fully converged to the correct channel. This is due to the fact that the matrices that the LMS method is based on are ill-conditioned. The block method uses singular value decomposition to overcome this limitation.

The next simulation was done under the same conditions except the value of the step size was changed to  $\mu = 3 \times 10^{-5}$  to determine the effect on the proposed algorithm. The results of this change can be seen in Figure 6. The proposed adaptive method works poorly compared to the block estimation method.

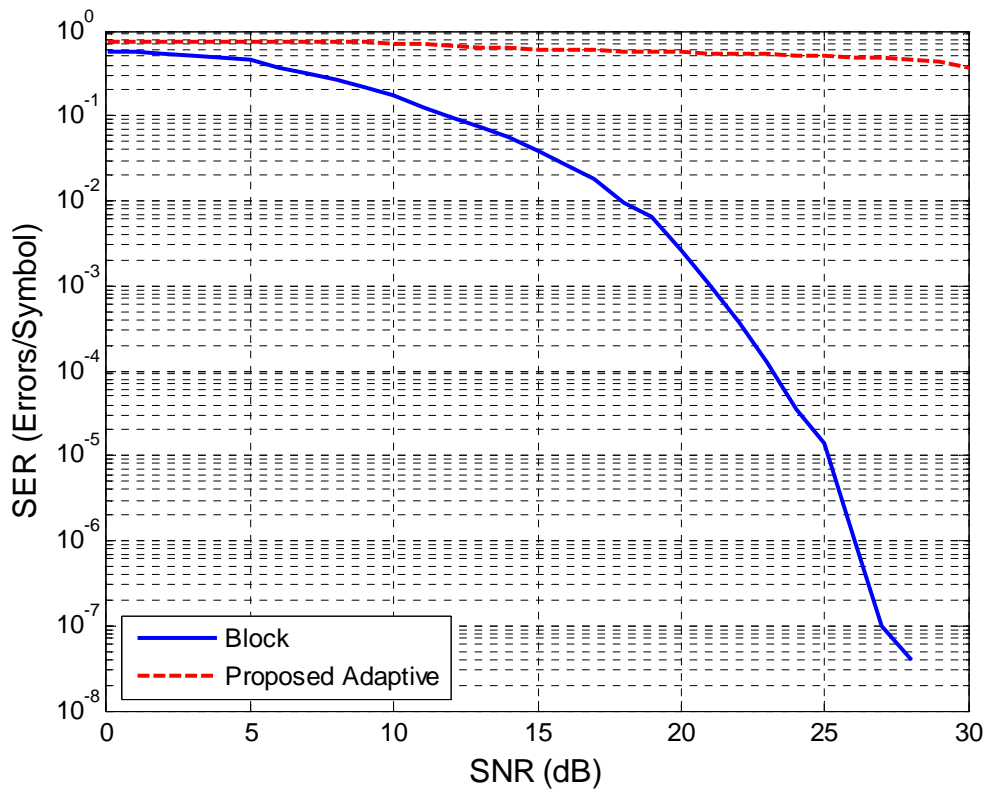


Figure 6. QPSK SER versus SNR with a step size of  $\mu = 3 \times 10^{-5}$ .

## 2. Non-Stationary Channel Performance

The next test of the proposed implementation was to examine the effect that a non-stationary channel has on its performance. The non-stationary channel was simulated using a basic random walk. The channel was initially a set of four complex impulses distributed within the length of the guard interval. Every OFDM symbol, this channel was updated to a new value by a random walk. The random walk step size has been calculated as a percent of the channel power. The channel coefficients are obtained iteratively from

$$C_{i+1} = C_i + \beta E[C_i^2] \Delta C \quad (75)$$

where  $\Delta C$  is a random vector consisting of  $[1, 0, -1]$ ,  $\beta$  is a scaling factor, and  $E[C_i^2]$  is the channel power.

The block method of channel estimation was expected to perform poorly, based on the fact that it assumes a stationary channel over the entire data set of 10000 received blocks. With the small LMS step size  $\mu = 10^{-7}$ , the adaptive method performed comparable to the block method. The small step size affected its ability to converge on the actual channel estimate as each OFDM symbol was received.

To ensure that the poor performance was due to the LMS step size, the simulation was also run using  $\mu = 3 \times 10^{-5}$ . The results of this simulation are shown in Figure 7, where SNR is defined in Section 1 of this chapter.

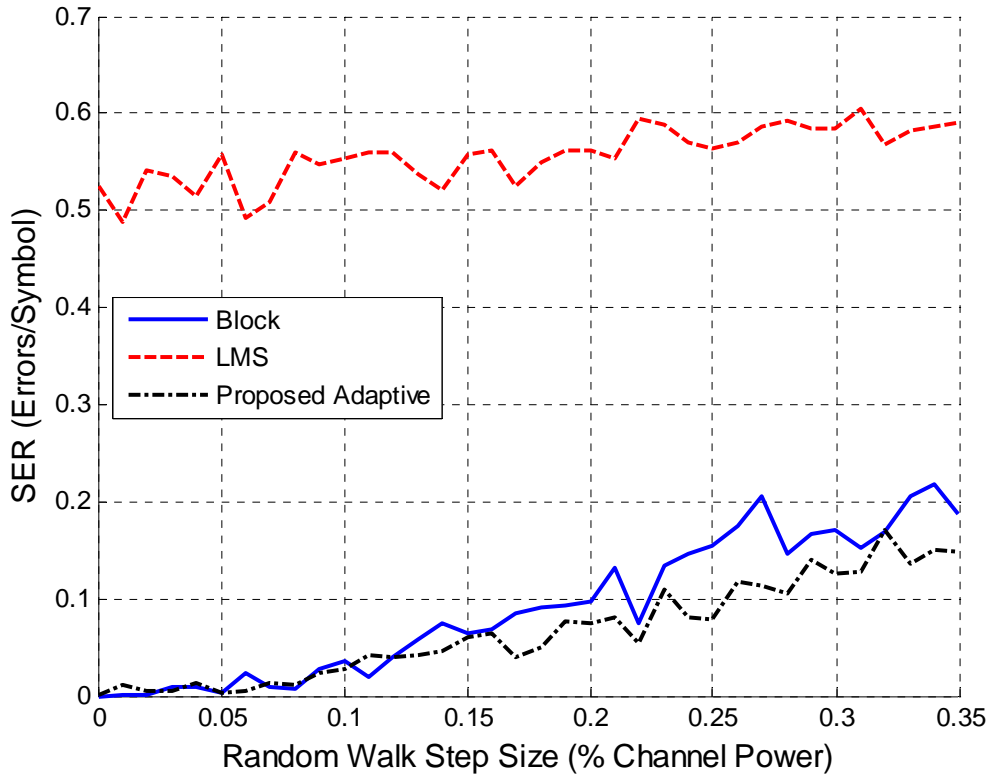


Figure 7. QPSK SER versus random walk step size with an LMS step size of  $\mu = 3 \times 10^{-5}$ .

As illustrated in Figure 7, the LMS method based on the blind equalization algorithm in Chapter III is very sensitive to the LMS step size. The proposed DFT based adaptive method performs better than the block method and the Chapter III LMS method fails to converge to a solution. The step size for the proposed DFT based adaptive method can be adjusted to give faster convergence on a non-stationary channel; however, the gains are marginal, since the block method reaches 10% SER for a random walk step size of 0.21 percent of channel power, while the alternative LMS method reaches 10% SER at 0.23 percent. This can also be seen in Figure 8, where the alternative LMS method and block method have been plotted using a logarithmic scale. The error rate for the block method is better than that of the alternative LMS method until a random walk step size of 0.08 percent of the total channel power is reached. Although there are several

data points at which the block method outperforms the alternative LMS method above 0.08 percent, in general, the alternative LMS performs better.

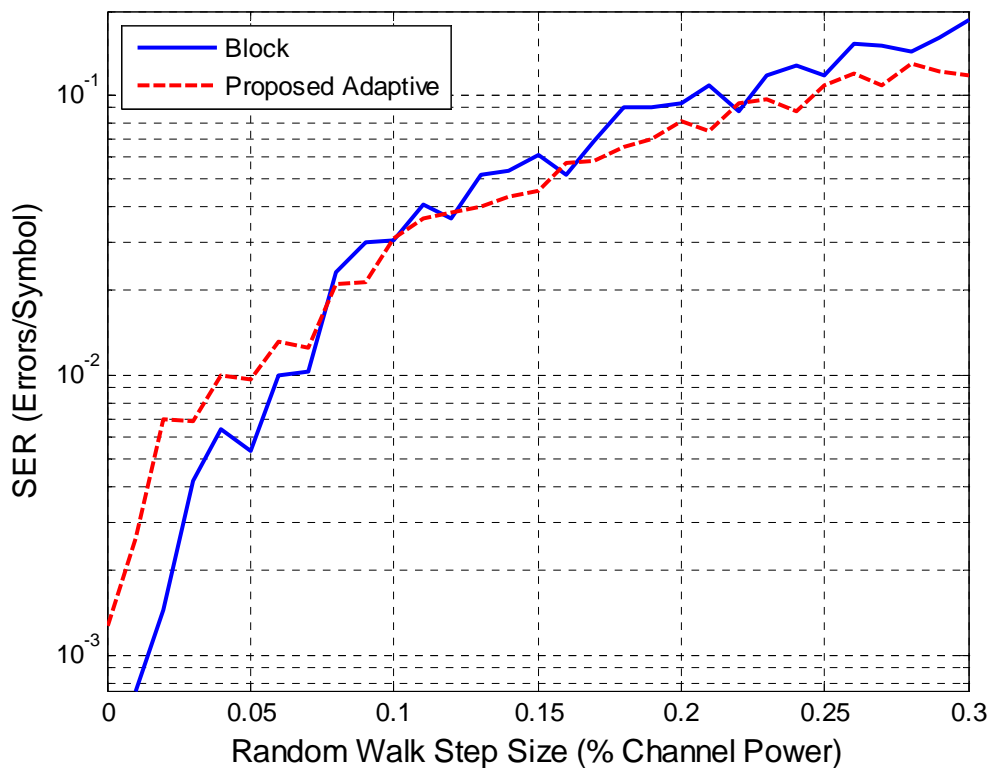


Figure 8. A comparison of the block and proposed adaptive method of calculating the channel using a step size of  $\mu = 3 \times 10^{-5}$ . These results were generated using 500 trials at each data point.

These results also fail to take into account the fact that the larger step size affects the performance in AWGN, as seen in Section 1.

### 3. Effects of Errors in the Initial Channel Estimate

The simulations performed in the preceding sections assumed that there was a perfect initial estimate of the channel conditions based on the reception of a preamble. The performances of the algorithms based on a poor initial channel estimate are investigated in this section. Only the two LMS-based methods are tested in this section since the block method does not rely on an initial channel estimate. The error in the

initial estimate was simulated by taking the original channel estimate and multiplying each frequency of the channel by a different random real number. The initial estimate is given by:

$$C_{init,j} = C_{act,j}v_j \quad (76)$$

where  $C_{init}$  is the channel estimate given to the simulation,  $C_{act}$  is the actual channel impulse response, and  $v_j \sim N(1,r)$  with  $r$  defined as the seed channel variance. The performance metric for this algorithm was based on the number of OFDM symbols it took for the algorithm to converge to less than a 10% SER. This was calculated by running the algorithm until an OFDM symbol had five or less errors in it. The number of symbols was still set to 10,000, and if the algorithm failed to converge by then, it was assumed that it would not converge. The results of this simulation are seen in Figure 9.

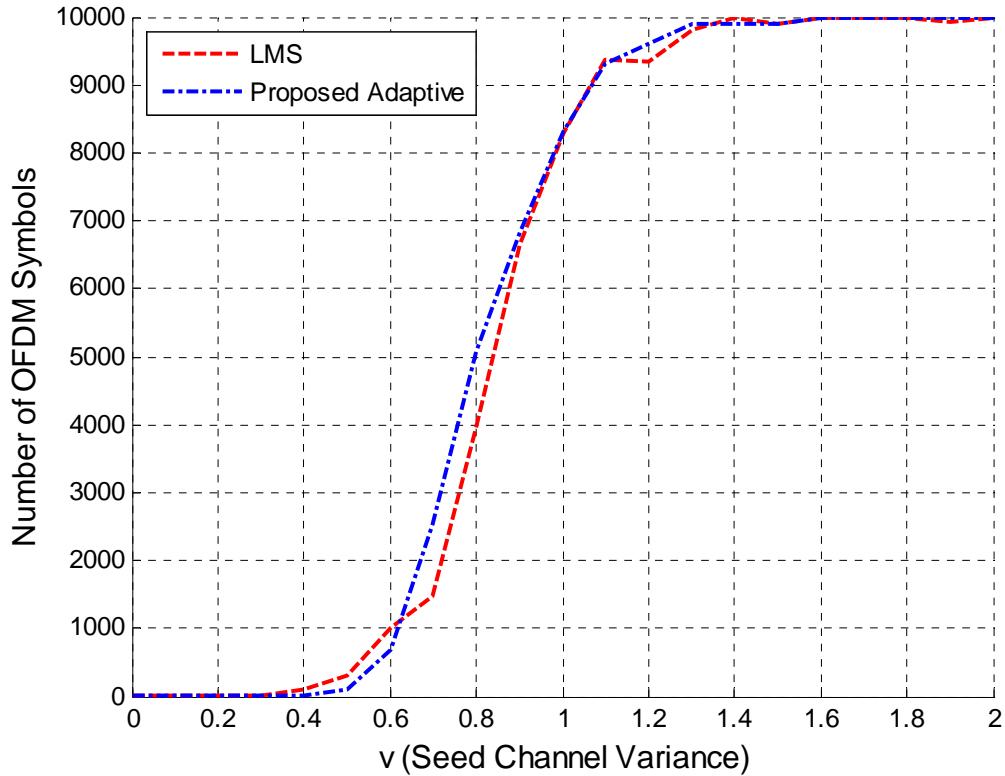


Figure 9. Number of OFDM symbols required to converge versus seed channel variance for a step size of  $\mu = 10^{-7}$ .

Both algorithms perform poorly at the lower step size of  $\mu = 10^{-7}$ , taking over 8,000 blocks to converge at a seed channel variance of 1.0 and failing to converge beyond a seed channel variance of 1.4. Assuming a OFDM symbol interval of  $4.0 \mu\text{s}$ , based on IEEE Standard 802.11a, we find that this translates to a convergence time of 32 ms.

The step size was then increased to  $\mu = 3 \times 10^{-5}$  to see what effect, if any, it had on the convergence of the two algorithms. It can be seen in Figure 9 that the alternative LMS method converges much faster than the original LMS method.

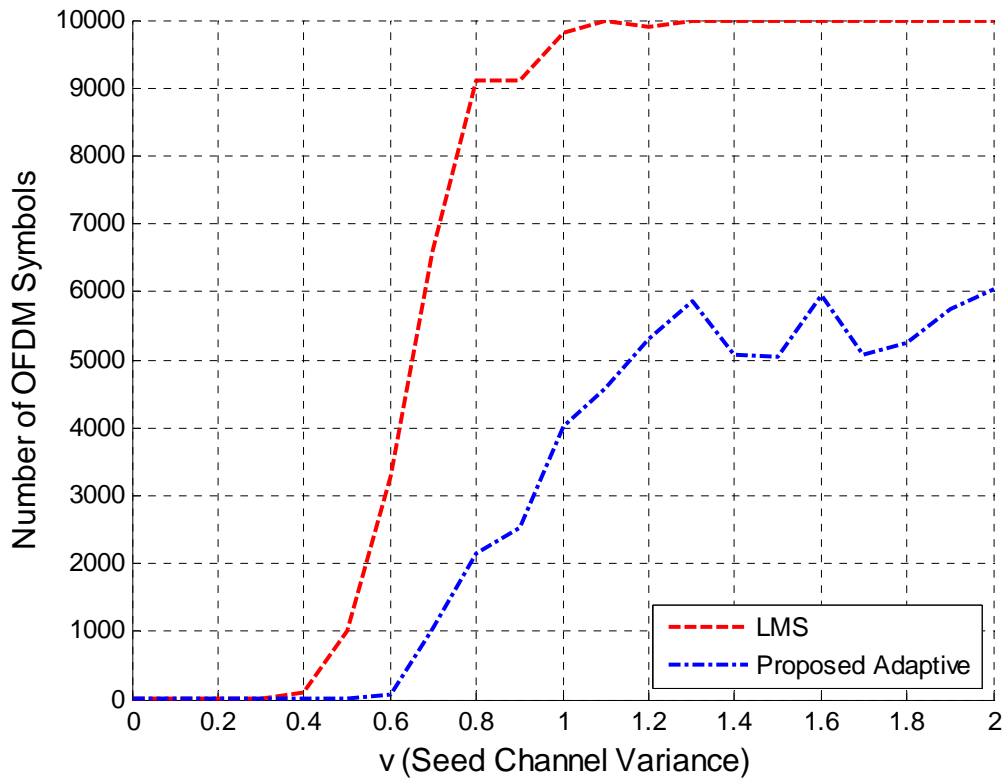


Figure 10. Number of OFDM symbols required to converge versus seed channel variance for a step size of  $\mu = 3 \times 10^{-5}$ .

With the larger step size, the alternative LMS method converges between 20 and 24 ms for seed channel variances of 1.1 to 2.0. The original LMS method shows slightly degraded performance at the larger step size. Due to the fact that the algorithms do not always converge, the plot is not smooth through seed channel variances of 1.3 to 2.0.

This chapter investigated a DFT-based adaptive method for channel estimation. The next chapter discusses an algorithm for the estimation of data in null subchannels that is also based on the DFT.



THIS PAGE INTENTIONALLY LEFT BLANK

## V. DATA RECOVERY FROM A FADED SUBCARRIER

### A. PROPOSED NULL ESTIMATION METHOD

One of the issues in OFDM is the loss of data in subcarriers corresponding to nulls in the frequency response of the channel. This is particularly significant in environments with multipath, which adds destructively at certain frequencies. The method presented in this chapter is based on [10].

The argument of this section is that, using OFDM with ZP and an FFT size twice the OFDM symbol length, the even and odd subcarriers of the OFDM symbol offer sufficient redundancy so that the lost data can be recovered.

In order to introduce this concept, let the transmitted OFDM symbol be

$$x = [x[0], x[1], \dots, x[M-1], 0, \dots, 0] \quad (77)$$

where  $x$  is a vector of length  $P$ , which includes the ZP of  $L$  zeros at the end. Now define the  $M$  point DFT and the  $2M$  point (zero padded) DFT as

$$\begin{aligned} X_M[k] &= DFT \{ [x[0], \dots, x[M-1]] \}, \quad k = 0, \dots, M-1 \\ X_{2M}[m] &= DFT \{ [x[0], \dots, x[M-1], 0, 0, \dots, 0] \}, \quad m = 0, \dots, 2M-1 \end{aligned} \quad (78)$$

where  $M$  zeros are added to  $x$  before the  $2M$  point DFT is taken.

Then, as discussed in (66), for any odd  $k$  we can write

$$\sum_{\substack{l=0 \\ l \text{ even}}}^{2M-1} X_{2M}[l]W[k-l] + X_{2M}[k]W[0] = 0. \quad (79)$$

Since  $\ell$  is even and  $k$  is odd we can let  $k = 2m+1$  and rewrite this equation as

$$M \frac{Y[2m+1]}{C[2m+1]} = - \sum_{l=0}^{M-1} W[2(m-l)+1] X_M[l]. \quad (80)$$

Now, set an arbitrary threshold and use it to partition the transmitted data into two parts such that:

$$X[l] = X_+[l] + X_-[l] \quad (81)$$

with

$$\begin{aligned}
X_+[l] &= \begin{cases} X[l] & \text{if } |C[l]| > \text{Thresh} \\ 0 & \text{if } |C[l]| \leq \text{Thresh} \end{cases} \\
X_-[l] &= \begin{cases} X[l] & \text{if } |C[l]| \leq \text{Thresh} \\ 0 & \text{if } |C[l]| > \text{Thresh} \end{cases}
\end{aligned} \tag{82}$$

where *Thresh* is an arbitrary threshold.

In other words,  $X_-[\ell]$  indicates the subcarriers received at low power (at or close to a null in the channel) and  $X_+[\ell]$  all others.

Now, if the partitioned data is inserted into (80), it becomes

$$\frac{Y[2m+1]}{C[2m+1]} = \frac{1}{M} \sum_{l=0}^{M-1} W[2(m-l)+1]X_+[l] + \frac{1}{M} \sum_{l=0}^{M-1} W[2(m-l)+1]X_-[l]. \tag{83}$$

Define

$$\begin{aligned}
w_0[n] &= IDFT \{W[2k+1]\} = -e^{-j\frac{\pi}{M}n} \\
x_{\pm}[n] &= IDFT \{X_{\pm}[l]\}
\end{aligned} \tag{84}$$

Using the above definitions in (83), we get

$$\frac{Y[2k+1]}{C[2k+1]} = DFT \{w_0[n]x_+[n]\} + DFT \{w_0[n]x_-[n]\}. \tag{85}$$

If the term containing  $x_-[n]$  on the right hand side of the equation is isolated, then

$$DFT \{w_0[n]x_-[n]\} = \frac{Y[2k+1]}{C[2k+1]} - DFT \{w_0[n]x_+[n]\}. \tag{86}$$

If the inverse discrete Fourier transform (IDFT) of both sides of (86) is taken, then

$$w_0[n]x_-[n] = IDFT \left\{ \frac{Y[2k+1]}{C[2k+1]} \right\} - w_0[n]x_+[n]. \tag{87}$$

Now, dividing both sides by the  $w_0[n]$  term to solve for the terms of the transmitted signal below the threshold, we get

$$x_-[n] = \frac{1}{w_0[n]} IDFT \left\{ \frac{Y[2k+1]}{C[2k+1]} \right\} - x_+[n] \tag{88}$$

and, finally,

$$X_{-}[\ell] = DFT\{x_{-}[n]\}, \ell = 0, \dots, M - 1 \quad (89)$$

is the data recovered at, or close to, the nulls of the channel.

## **B. SIMULATION RESULTS**

To test the null estimation method described in Section A of this chapter, a test similar to those in Chapter IV were run, with several significant differences. Instead of using the OFDM symbol format described in IEEE Standard 802.11a, no nulls or pilots were included in the OFDM symbol. This was done in order to test the proposed concept of null estimation without having to worry about the effects of the nulls in the OFDM symbol. Additionally, knowledge of the channel was assumed.

The null estimation algorithm continued to use the delay of one block to achieve the effects of a ZP while transmitting the symbol with a CP. To test the algorithm, transmission was simulated over a noisy channel, where the noise was AWGN.

For testing, we used a family of random channels all with zero frequency response at a specific frequency  $\omega_0$ . An example channel response is shown in Figure 11.

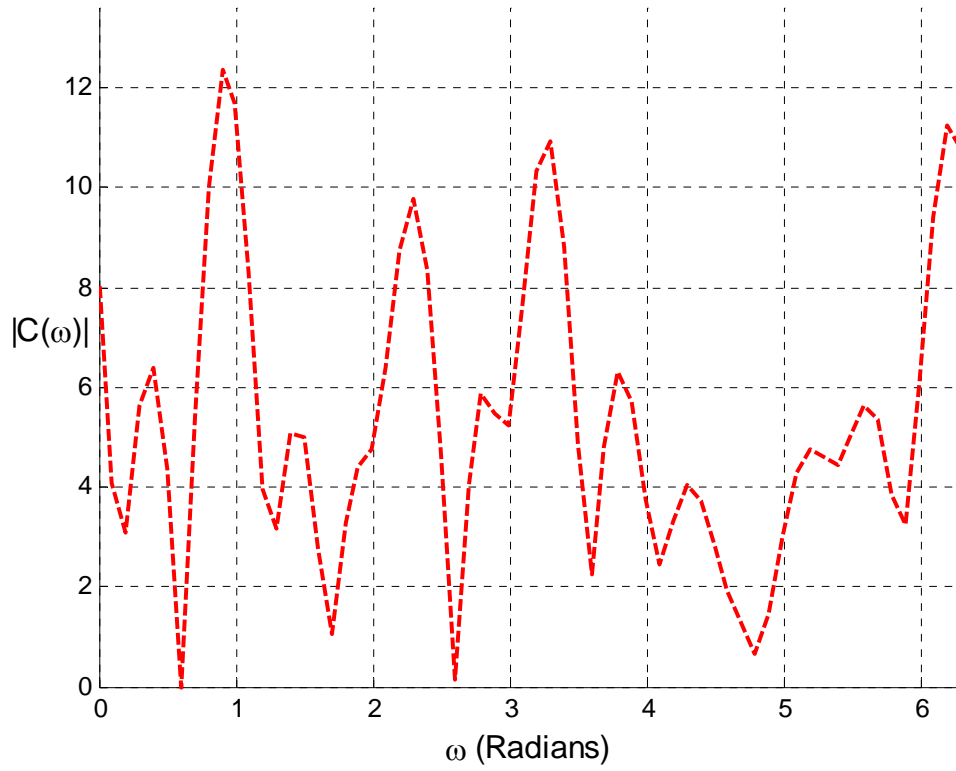


Figure 11. One of a family of channel frequency responses, all having nulls at  $\omega = 0.589$  radians.

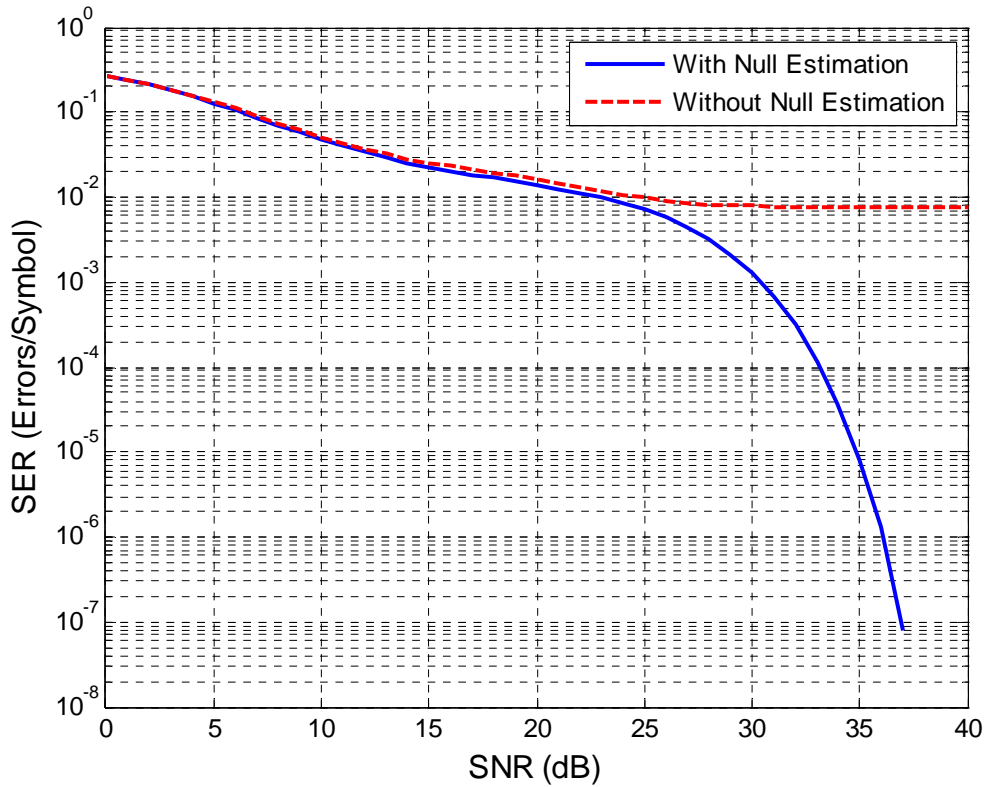


Figure 12. A comparison of the QPSK symbol error rate between a normal OFDM receiver algorithm and a null estimating OFDM receiver algorithm.

The performance of the standard algorithm (solid line) is compared with that of the proposed algorithm (dashed line) in terms of symbol error versus SNR in Figure 12. The two algorithms have similar performance up to 25 dB SNR, although the null estimating OFDM receiver algorithm performs slightly better overall. Above 25 dB SNR, there is a sharp drop in the error rate from the null estimation algorithm, while the normal OFDM receiver algorithm remains constant at  $7.8 \times 10^{-3}$  errors per symbol due to the information lost in the deep fading sub-carriers.

This chapter presented an algorithm for the estimation of the data lost in null subchannels and simulation results from the implementation of this algorithm. Chapter VI provides a summary of the work presented in this thesis, significant results, and recommendation for future work.

THIS PAGE INTENTIONALLY LEFT BLANK

## VI. CONCLUSION

The goal of this thesis was to investigate an adaptive implementation of the blind channel equalization method proposed in [1]. This adaptive method was implemented using the current OFDM symbol architecture from IEEE standard 802.11a. Once the adaptive method based on the work in [1] was simulated, an alternative method was developed with more robust performance characteristics. The algorithm for the second method led to the development of a proposed method of null channel estimation, which was also simulated in this thesis.

### A. SUMMARY

This thesis presented a subspace-based method of blind channel estimation of OFDM modulated signals that used the zero prefix as the guard band interval. Based on this, a method of adaptive blind channel estimation has been proposed. Furthermore, it is shown that the redundancy in ZP OFDM can be exploited to recover data from deeply faded subcarriers. The blind channel estimation methods were implemented in MATLAB and then compared for performance for several different channel conditions. Both a noisy channel with AWGN and a non-stationary channel were used to compare the results of the three methods of channel estimation. Additionally, two adaptive methods were tested in the presence of errors in the initial channel estimate to see if they could recover the original channel estimate.

Finally, the algorithm for data recovery from faded subcarriers was coded in MATLAB and simulated. Since in this case we assume full knowledge of the channel, it was only tested in a channel with AWGN. The results of this simulation were compared to those of an OFDM system that did not perform null estimation.

### B. SIGNIFICANT RESULTS

The method of blind channel estimation proposed in [1] can be implemented in an adaptive form. However, this method is very sensitive to the step size used in the LMS algorithm. The algorithm did not converge in a channel with AWGN with a relatively



large step size ( $\mu = 3 \times 10^{-5}$  in the example). Similarly, the algorithm performed poorly with this step size for both the non-stationary channel simulation and the incorrect initial channel estimate simulation.

The proposed adaptive method is more robust than the original. For the AWGN noisy channel with an LMS step size of  $\mu = 10^{-7}$ , the system converged to a lower error rate in simulated low SNR environments than the off-line, block method. This can be seen in Table 1.

Table 1. Comparison of calculated SER at various SNR for the blind estimation methods using a step size of  $\mu = 10^{-7}$ .

SNR (dB)	Block Method (Errors/Symbol)	Proposed DFT Based Adaptive Method (Errors/Symbol)
0	$5.799 \times 10^{-1}$	$4.543 \times 10^{-1}$
5	$4.513 \times 10^{-1}$	$2.090 \times 10^{-1}$
10	$1.741 \times 10^{-1}$	$6.203 \times 10^{-2}$
15	$3.895 \times 10^{-2}$	$2.155 \times 10^{-2}$
20	$2.640 \times 10^{-3}$	$5.982 \times 10^{-3}$
25	$1.390 \times 10^{-5}$	$4.837 \times 10^{-4}$

With the larger step size, the block method outperforms the adaptive LMS algorithm. However, there are several advantages to the larger LMS step size, which can be seen in the results from the other two simulations. The alternative adaptive method with the larger step size outperforms the block algorithm during the non-stationary channel simulation above a random walk step size of 0.08 percent of channel power by an average of 0.0175 symbol errors/symbol. For the bad initial channel estimation simulation, the larger LMS step size outperforms the smaller step size significantly, which can be seen in Table 2.

Table 2. Comparison of convergence speed for various seed channel variances for the original and alternative adaptive methods with an LMS step size of  $\mu = 3 \times 10^{-5}$ .

Seed Channel Variance	Adaptive Method (Number of OFDM Symbols)	Alternative Adaptive Method (Number of OFDM Symbols)	Time Difference (ms)
0	1	1	0
0.5	1001	4.25	4
1.0	9800	4009	23.2
1.5	Fails to Converge	5049	$\infty$
2.0	Fails to Converge	6031	$\infty$

Perhaps the most significant result is the fact that the proposed adaptive method can be tuned for performance based on the channel conditions that may exist.

The recovery of data transmitted over deep fading channels was shown to be possible using the algorithm described in Chapter V. For relatively high SNR (25 dB in this example), the proposed algorithm clearly outperformed the standard receiver which cannot recover the faded data.

### C. RECOMMENDATIONS FOR FUTURE WORK

There are numerous areas available for future work with this thesis. First, the proposed algorithm should be evaluated using actual channel characteristics to determine if it is viable for use in an actual communication method.

Secondly, the adaptive method should be tuned to perform based on channel characteristics. In a normal OFDM modulation scheme, such as IEEE Standard 802.11a, a known preamble is sent before data transmission begins. The channel characteristics

determined from the preamble should then be used to determine the desired LMS step size. By modifying the step size, the performance of the algorithm can be enhanced for noisy or non-stationary channels.

Third, the null estimation algorithm should be tested using an OFDM symbol from a current standard and integrated with channel estimation method. If knowledge of the channel were known before transmission, no data would be sent over channels with deep fading. Once a channel has been determined to have sub-carriers with deep fading characteristics, null estimation should be performed to determine if the algorithm will perform as well with only an estimation of the channel characteristics.

## LIST OF REFERENCES

- [1] P. P. Vaidyanathan and B. Vrcelj, "A frequency domain approach for blind identification with filter bank precoders," in *Proc. 2004 Int. Symp. Circuits and Systems*, pp. III- 349–52, 2004.
- [2] Cisco Systems. (2011, February 1). *Cisco Visual Networking Index: Global Mobile Data Traffic Forecast Update, 2010–2015* [Online]. Available: [http://www.cisco.com/en/US/solutions/collateral/ns341/ns525/ns537/ns705/ns827/white\\_paper\\_c11-520862.html](http://www.cisco.com/en/US/solutions/collateral/ns341/ns525/ns537/ns705/ns827/white_paper_c11-520862.html).
- [3] J. G. Andrews et al., *Fundamentals of WiMAX*. San Francisco, CA: Prentice Hall, 2007.
- [4] R. Cristi, unpublished notes, March 2010.
- [5] P. P. Vaidyanathan and B. Su, "Remarks on certain new methods for blind identification of FIR channels," in *Conf. Rec. 38<sup>th</sup> Asilomar Conf. Signals, Systems and Computers*, Asilomar, CA, pp. I- 832–836, 2004.
- [6] Supplement to IEEE Standard for Information technology- Telecommunications and information exchange between systems- Local and metropolitan area networks- Specific requirements- Part 11: Wireless LAN Medium Access Control (MAC) and Physical Layer (PHY) specifications: High-speed Physical Layer in the 5 GHz Band, IEEE Standard 802.11a-1999, 1999.
- [7] R. Cristi, unpublished notes, April 2010.
- [8] IEEE Standard for Information technology- Telecommunications and information exchange between systems- Local and metropolitan area networks- Specific requirements- Part 11: Wireless LAN Medium Access Control (MAC) and Physical Layer (PHY) Specifications Amendment 5: Enhancements for Higher Throughput, IEEE Standard 802.11n-2009, 2009.
- [9] R. Cristi, unpublished notes, September 2010.
- [10] R. Cristi, unpublished notes, October 2010.

THIS PAGE INTENTIONALLY LEFT BLANK

## INITIAL DISTRIBUTION LIST

1. Defense Technical Information Center  
Ft. Belvoir, Virginia
2. Dudley Knox Library  
Naval Postgraduate School  
Monterey, California
3. Professor R. Clark Robertson  
Chairman Code EC  
Department and Electrical and Computer Engineering  
Monterey, California
4. Professor Roberto Cristi  
Department and Electrical and Computer Engineering  
Monterey, California
5. Professor Frank Kragh  
Department and Electrical and Computer Engineering  
Monterey, California
6. Donna Miller  
Department of Electrical and Computer Engineering  
Monterey, California
7. Professor Tri Ha  
Department of Electrical and Computer Engineering  
Monterey, California
8. Lieutenant Anthony Stranges  
Department of Electrical and Computer Engineering  
Monterey, California